

Electron-Capture Decay Rate of  ${}^7\text{Be}$  Encapsulated in  $\text{C}_{60}$  CagesT. Ohtsuki,<sup>\*,a</sup> K. Hirose,<sup>a</sup> and K. Ohno<sup>b</sup><sup>a</sup>Laboratory of Nuclear Science, Tohoku University, Mikamine, Taihaku, Sendai 982-0826, Japan<sup>b</sup>Department of Physics, Yokohama National University, 79-5 Tokiwadai, Hodogaya-ku, Yokohama 240-8501, Japan

Received: March 30, 2007

The decay rate of  ${}^7\text{Be}$  electron capture (EC) was measured in  $\text{C}_{60}$  and Be metal with a reference method. The half-lives of  ${}^7\text{Be}$  endohedral  $\text{C}_{60}$  ( ${}^7\text{Be}@C_{60}$ ) and  ${}^7\text{Be}$  in Be metal (Be metal( ${}^7\text{Be}$ )) were found to be  $52.65 \pm 0.04$  and  $53.25 \pm 0.04$  days, respectively. This amounts to a 1.13% difference in the EC-decay half-life between  ${}^7\text{Be}@C_{60}$  and Be metal( ${}^7\text{Be}$ ). The result is a reflection of the different electron wave-functions for  ${}^7\text{Be}$  inside  $\text{C}_{60}$  compared to when  ${}^7\text{Be}$  is in a Be metal. Here, the magnitude of the average charge-transfer from the L(2s) electrons of the  ${}^7\text{Be}$  atom plays an important role in such variation in the decay constant in the environments.

## 1. Introduction

In nuclear  $\beta$ -decay and in the closely related process of electron-capture(EC), the decay curve is an exponential function versus time with a constant decay rate. The decay rate from any parent state, usually the nuclear ground state, to any final daughter state is proportional to the product of a nuclear matrix element and factors related to the phase-space available to the neutrino and electron and to the overlap between the initial electron and final nuclear wave functions. As first suggested by Segrè et al.,<sup>1-3</sup> environmental factors such as the chemical form and pressure, among others, may alter the electron contact densities in the nucleus and thus affect the EC decay rates. In this regard, the nucleus of  ${}^7\text{Be}$  is a good candidate to look for such variations in environmental factors because of its simple electronic structure,  $1s^2 2s^2$ , in the EC decay nucleus.<sup>4-9</sup>

A long-standing challenge has been to establish the degree to which manipulation of these environmental factors can in practice change nuclear decay rates in experiments to determine the decay rate of  ${}^7\text{Be}$  compounds. In addition, there have been several observations of variations in the half-life with host metals,<sup>10-19</sup> chemical forms,<sup>20-23</sup> and pressure.<sup>24-26</sup> For example, we introduce, in Figures 1 and 2, the variations of the half-life in chemical form and pressure were presented by Jolidge et al<sup>21</sup> in 1970 and Hensley et al<sup>24</sup> in 1973. From the early data, the half-life variations of  ${}^7\text{Be}$  as a function of different chemical

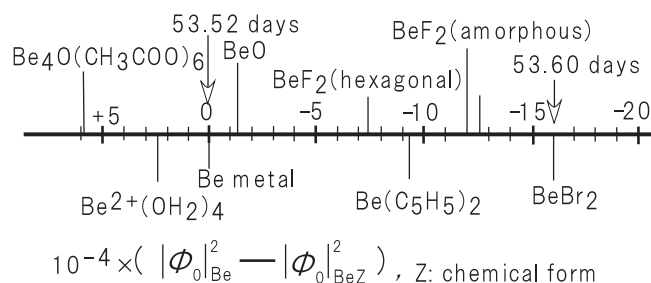


**Figure 1.** Differences of electron densities at the Be nucleus in various compounds ( $\text{BeZ}$ ) of Be. The difference of horizontal value in units of  $10^{-4} \times |\phi_0|^2_{\text{Be}}$ .

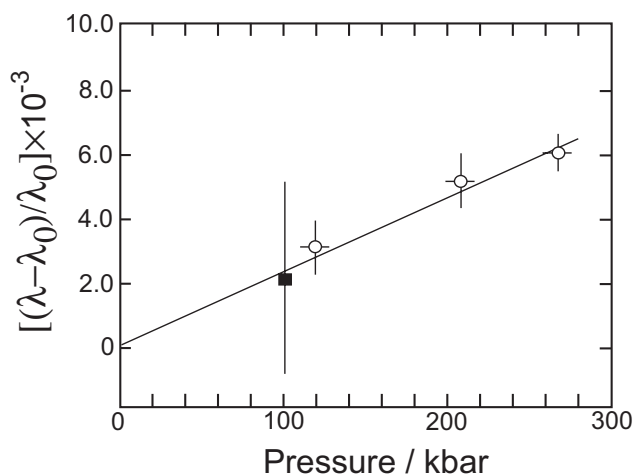


**Figure 2.** Pressure dependence of the half-life in the chemical form of  ${}^7\text{BeO}$ . The half-life of  ${}^7\text{Be}$  in  ${}^7\text{BeO}$  at 1 kbar (normal pressure) corresponds to 53.41 days. Open circles are the data presented by Hensley et al.<sup>24</sup> and a closed square is by Gogarty.<sup>26</sup>

forms and host materials have been limited almost to within 0.2%, (and even under high pressure up to 270 kbar, to within 0.59%<sup>24</sup>). Other summaries of the early studies in the EC decay are also given by Emery.<sup>27</sup> In recent studies, however, large variations have been observed as a function of different chemical forms and pressures.<sup>16, 20, 25</sup> Therefore, a precise measurement is still needed to obtain the absolute decay rate in different circumstances.

After the discovery of  $\text{C}_{60}$  and the subsequent successful production of several kinds of fullerenes,<sup>28, 29</sup> endohedral fullerenes which have one or more atoms inside the  $\text{C}_{60}$ ,  $\text{C}_{70}$ ,  $\text{C}_{82}$  cages etc. currently have attracted great interest.<sup>30, 31</sup> If their mass production becomes possible, they would have many interesting applications such as stable molecular devices in nano-meter scales and/or as functionalized materials in many fields. Although endohedral complexes can be created simultaneously as well as ordinary fullerenes by using arc-discharge vaporization of composite rods made of graphite and metal compounds, the production rate of endohedral  $\text{C}_{60}$  is quite low compared to ordinary  $\text{C}_{60}$ . An alternative way of producing endohedral  $\text{C}_{60}$  is to insert foreign atoms into the cage of the preexisting  $\text{C}_{60}$  afterwards.<sup>32-34</sup> We have examined the forma-

\*Corresponding author. E-mail: ohtsuki@LNS.tohoku.ac.jp

tion of endohedral fullerenes by a nuclear recoil implantation of several foreign atoms following nuclear reactions.<sup>35-39</sup> We found that the  $^7\text{Be}$  atom can be endohedrally doped to create the  $^7\text{Be}$  endohedral  $\text{C}_{60}$  ( $^7\text{Be}@\text{C}_{60}$ ).<sup>36</sup>

Because of the unique chemical form of  $\text{C}_{60}$  and/or several factors contributing to this environment; many  $\pi$  electrons of  $\text{C}_{60}$ , and special dynamic motions inside  $\text{C}_{60}$  etc.,<sup>40-42</sup> the electron contact density on the  $^7\text{Be}$  nuclei can be affected significantly by the electron environment of  $\text{C}_{60}$ . Therefore, it is intriguing to measure the half-life of the  $^7\text{Be}$  inside  $\text{C}_{60}$ ; "how does the EC decay rate of  $^7\text{Be}$  change inside the  $\text{C}_{60}$  cage relative to other situations?" We compared the half-life of  $^7\text{Be}$  when it is encapsulated in a  $\text{C}_{60}$  cage to that in Be metal as a reference. In order to accurately calibrate our time measurements we relied on a standard clock time radio signal. We found a surprisingly shorter half-life of  $^7\text{Be}$  inside  $\text{C}_{60}$ .<sup>43</sup> This fact implied that the  $^7\text{Be}$  atoms are located in a unique environment inside  $\text{C}_{60}$ .

## 2. Experimental procedures and simulation

**2.1. Preparation of  $^7\text{Be}@\text{C}_{60}$ .** A nuclear recoil implantation technique was used to produce  $^7\text{Be}@\text{C}_{60}$ . Purified fullerene ( $\text{C}_{60}$ ) and  $\text{Li}_2\text{CO}_3$  were used in powder form. The grain size of the material was smaller than 100 mesh (20  $\mu\text{m}$ ) for  $\text{Li}_2\text{CO}_3$ . Fullerene  $\text{C}_{60}$  was carefully mixed with  $\text{Li}_2\text{CO}_3$  (weight ratio=1:1) in an agate mortar, and a few mL of carbon disulfide ( $\text{CS}_2$ ) was added. After the mixture dried, about 100 mg of the mixed sample was pressed into a tablet and wrapped in a pure aluminum foil of 10  $\mu\text{m}$  in thickness for irradiation. Proton irradiation with a beam energy of 16 or 18 MeV was performed at the Cyclotron and Radioisotope Center, Tohoku University. The beam current was typically 3  $\mu\text{A}$  and the irradiation time was about 24 hours. The sample was cooled with a He-gas during irradiation. The  $^7\text{Li}(p,n)^7\text{Be}$  reaction leads to the production of  $^7\text{Be}$ . After the kinetic energy of  $^7\text{Be}$  has decreased in the sample (target) to an appropriate value, it then penetrates into the  $\text{C}_{60}$  cage to produce the endohedral fullerene (a nuclear recoil implantation, the detailed mechanism of which is shown in Figure 3).

After irradiation, the sample was left for a few days to allow several kinds of short-lived radioactive by-products to decay. The sample was dissolved in *o*-dichlorobenzene and filtered through a millipore filter (pore size=0.2  $\mu\text{m}$ ) to remove insoluble materials. The soluble portion was injected into a high performance liquid chromatography (HPLC) device equipped with a 5PBB (Cosmosil) (silica-bonded with a pentabromobenzyl group) column of 10 mm in inner diameter and 250 mm in length at a flow rate of 2 or 3 mL/min. To confirm the pres-

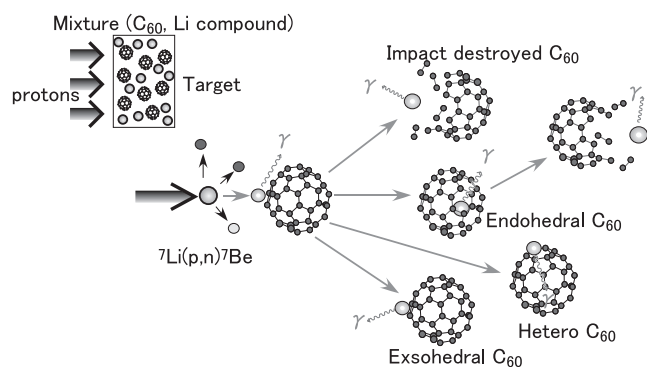


**Figure 3.** Schematic view of production mechanism for radioactive fullerenes.  $^7\text{Be}$  nuclide is produced by (p,n) reaction, and its kinetic energy of  $^7\text{Be}$  is reduced in the sample to a magnitude which is appropriate for the fusion. Finally,  $^7\text{Be}$  hits the  $\text{C}_{60}$  cages and stops in the cages.

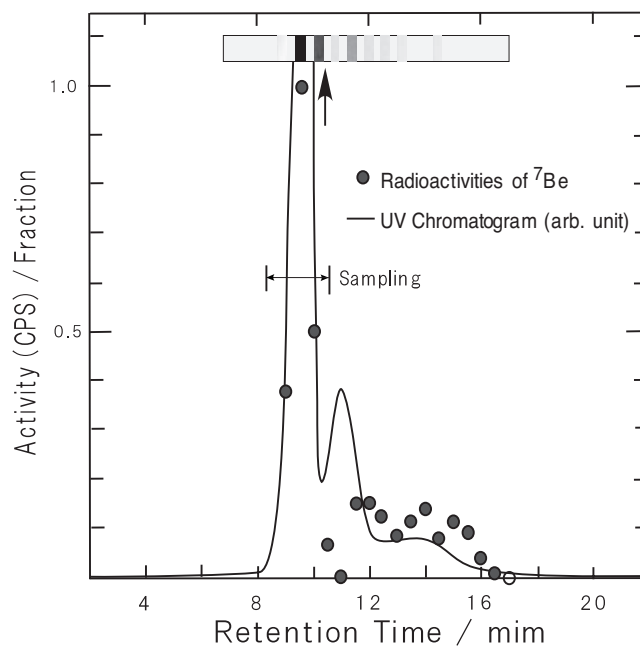


**Figure 4.** HPLC elution curves of the soluble portion of the crude extracted in the proton-irradiated sample of  $^7\text{Li}$  and  $\text{C}_{60}$ . The vertical axis indicates the radioactivities of  $^7\text{Be}$  in each fraction (solid circles) and absorbance of the UV chromatogram of  $\text{C}_{60}$ .

ence of fullerenes and their derivatives, a UV detector was installed with a wavelength of 290 nm. In order to prepare the sample of  $^7\text{Be}@\text{C}_{60}$ , eluent fractions were collected for 30 s intervals (0–30, 30–60, 60–90, ... s), and the 478 keV  $\gamma$ -ray activities emanating from the  $^7\text{Be}$  of each fraction were measured with a  $\gamma$ -ray detector for confirmation of the  $^7\text{Be}$  inside the  $\text{C}_{60}$  fraction. The eluent behavior is shown in Figure 4 and the solid circles in the figure show the results of the  $\gamma$ -ray measurements for each fraction. The horizontal axis represents the retention time (in min), which corresponds to each fraction collected at 30 s intervals, after injection into the HPLC. The vertical axis represents the counting rates of the 478 keV  $\gamma$ -ray from  $^7\text{Be}$ . One strong peak of  $^7\text{Be}$ -radioactivity was observed in the retention of 8.5–10 min. Radioactivities of  $^7\text{Be}$  on the fraction were estimated to be of the magnitude of 20–30 Bq/mg. The solid curve in Figure 4 indicates the absorbance monitored by a UV detector for the dissolved sample. A strong peak was also observed in the elution curve, though the relatively smaller peaks were also seen in 10–16 min. This peak position corresponds to the retention time of  $\text{C}_{60}$  which was confirmed by the calibration run using the  $\text{C}_{60}$  sample before the irradiation. Furthermore the second and third peaks were also attributed to  $\text{C}_{60}$  dimers and trimers, respectively, produced by coalescence reactions.

It was noted that the peak position of  $^7\text{Be}$  (solid circles) exactly coincided with the UV chromatogram of  $\text{C}_{60}$ . From the correlation of the elution behavior between the UV chromatogram and the radioactivities of the  $^7\text{Be}$  atoms, we found that the atom-doped fullerene,  $^7\text{Be}@\text{C}_{60}$ , was indeed produced by nuclear recoil implantation. In order to obtain a measurement sample, the solution which corresponded to a  $\text{C}_{60}$  fraction was evaporated, and finally the  $\text{C}_{60}$  sample containing  $^7\text{Be}@\text{C}_{60}$  was converted to a solid tablet by press.

**2.2. Simulation of  $^7\text{Be}@\text{C}_{60}$ .** In order to check the implantation procedure, an *ab initio* molecular dynamics (MD) simulation, based on all-electron mixed-basis approach with the framework of the local density approximation, was carried out for collision between the  $^7\text{Be}$  atom and  $\text{C}_{60}$  cage.<sup>44,45</sup> We put one  $\text{C}_{60}$  molecule and one Be atom in a supercell with zero and 5 eV initial kinetic energies for  $\text{C}_{60}$  and Be, respectively. The wave functions were expanded by 300 Slater-type atomic orbit-

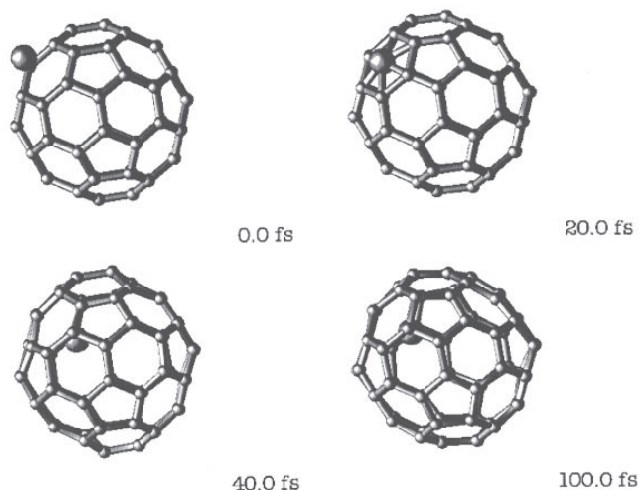


**Figure 5.** Time-ordered snapshots of a simulation,<sup>36</sup> where Be atom hits with 5 eV kinetic energy the center of a six-membered ring of  $\text{C}_{60}$ . In this case,  ${}^7\text{Be}@{}_{\text{C}_{60}}$  is created.

als and 2969 plane waves. The supercell was divided into  $64 \times 64 \times 64$  meshes with 2.7 meshes corresponding to 1 a.u. = 0.5918 Å. We performed six steepest-descent iterations between two adjacent updates of atomic positions in order to converge the electronic states, and choose  $\delta t = 4$  a.u. ~ 0.1 fs as the basic time step. For rescaling velocity and assuming a Fermi-Dirac distribution of electronic states, the simulation temperature of the whole system was set to be  $T = 1000$  K. In the case where a Be atom with 5 eV kinetic energy hits the center of a six-membered ring of  $\text{C}_{60}$  perpendicularly, we found that the Be atom easily penetrated into the cage through the center of the six-membered ring. It was trapped at 1.0 Å depth from the center of the same six-membered ring toward the cage center; see Figure 5. The reason why the insertion proceeded very easily is that the ionic radius of the Be atom is 0.45 Å, much smaller than the radius of the hole of a six-membered ring. If a Be atom with the same kinetic energy hits a C-C bond of a  $\text{C}_{60}$  atom, the bombardment gives a considerable shock and deformation to the  $\text{C}_{60}$  cage. If a Be atom with higher kinetic energy, e.g. 100 eV, hits a  $\text{C}_{60}$  molecule at any location, we found that the  $\text{C}_{60}$  cage was damaged considerably. These results suggest the following scenario of the present experiment: Many  $\text{C}_{60}$  cages are destroyed before the  ${}^7\text{Be}$  atoms have lost their kinetic energies during the recoil process in the sample, and once sufficiently low kinetic energies are reached, the insertion process  ${}^7\text{Be} + \text{C}_{60} \rightarrow {}^7\text{Be}@{}_{\text{C}_{60}}$  occurs. The snapshots of the simulation are shown in Figure 5.

**2.3. Preparation of Be metal ( ${}^7\text{Be}$ ).** The EC decay rate of the  ${}^7\text{Be}$  nucleus inside the Be metal (Be metal ( ${}^7\text{Be}$ )) have never been surveyed to date. Therefore, it would be interesting to measure the decay rate in the Be metal (uniform lattice structure, (hcp). In the present study, we measured the half-life of  ${}^7\text{Be}$  inside Be metal ( ${}^7\text{Be}$ ) for reference use compared to that of the  ${}^7\text{Be}@{}_{\text{C}_{60}}$  sample. Be metal (10 mm in diameter and 0.3 mm in thickness) was utilized to produce  ${}^7\text{Be}$  uniformly in a Be metal. After being washed with a diluted HCl solution, the Be metal was sealed in a quartz tube (vacuum packed) 12 mm in diameter to be used as a target. Irradiation with a bremsstrahlung (50 MeV electrons) was carried out by the electron linear accelerator, Laboratory of Nuclear Science, Tohoku University. The sample in a quartz tube was set in the middle path of a sweep magnet placed on the axis of the electron beam. A platinum plate converter with a thickness of 2 mm was set in front of the sweep magnet in order to generate the bremsstrahlung. Then the sample was irradiated only by the bremsstrahlung in such a way that all the electrons were removed by the

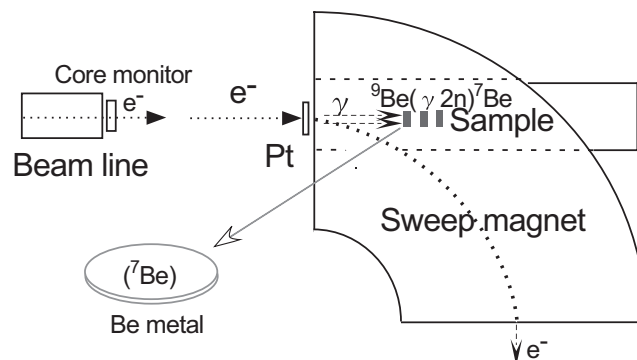


**Figure 6.** Setup for the irradiation of a Be metal using the electron linear accelerator at Tohoku University.

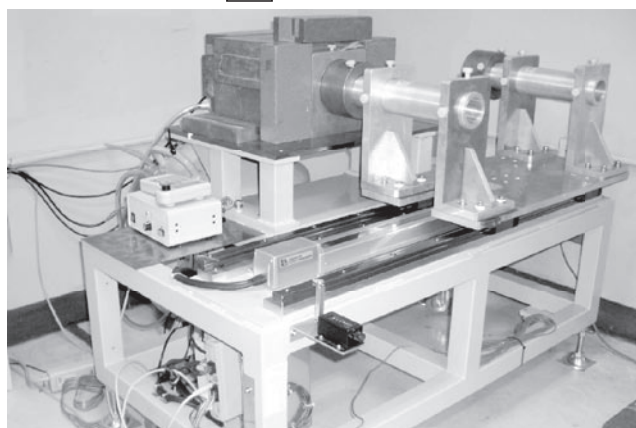
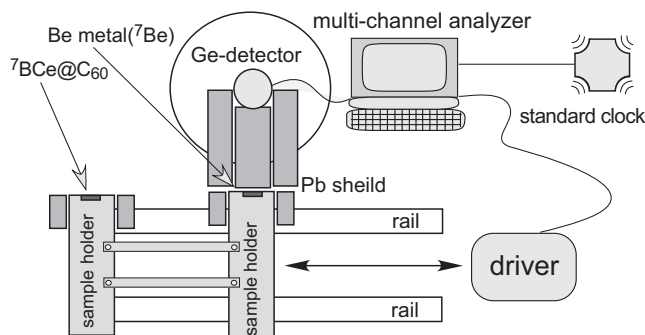


**Figure 7.** The measurement system: a computer-controlled sample changer. Two samples,  ${}^7\text{Be}@{}_{\text{C}_{60}}$  and Be metal ( ${}^7\text{Be}$ ), were placed on top of two arms of an automated sample changer, which moved the samples horizontally in front of a  $\gamma$ -ray detector. A computer clock was always calibrated by a standard clock time radio signal.

magnetic field. Therefore, damage to the lattice of the Be metal was confined to a minimum. The experimental setup for the irradiation procedure is shown in Figure 6. The  ${}^7\text{Be}$  can be produced uniformly by the  ${}^9\text{Be}(\gamma, 2n){}^7\text{Be}$  reaction in the Be metal. After the irradiation, the sample (Be metal ( ${}^7\text{Be}$ )) was baked in an electric oven with vacuum packing at 1150 °C (the melting point of Be metal is 1278 °C) for over one hour to recover a lattice defect caused by the  $(\gamma, 2n)$  reaction. Finally, the Be metal ( ${}^7\text{Be}$ ) was washed again with a diluted HCl solution to clean the surface.

**2.4.  $\gamma$ -Ray measurement by the reference method.** We developed a reference method to measure the half-life of  ${}^7\text{Be}$  inside  $\text{C}_{60}$  and that in the Be metal. The system is shown in Figure 7. This allowed the decay rates of the two samples to be measured in a comparable way. Two samples of the  ${}^7\text{Be}@{}_{\text{C}_{60}}$  and the Be metal ( ${}^7\text{Be}$ ) were placed on top of two arms of an automated sample changer, which moved the samples horizontally in front of a  $\gamma$ -ray detector.

The  ${}^7\text{Be}$  decays directly to a  $3/2^-$  ground state of  ${}^7\text{Li}$  with a branching of 89.6%; it goes with a branching of 10.4% to a first

excited state of  ${}^7\text{Li}(1/2^-$  at 478 keV), which decays by  $\gamma$ -ray emission to the ground state.<sup>46</sup> Therefore, the activities associated with  ${}^7\text{Be}$ , in particular the 478 keV  $\gamma$ -rays emanating from the EC-decay daughter of  ${}^7\text{Be}$ , were measured with a high-purity germanium (HPGe) detector ( $\Delta E_{\text{FWHM}}$  is 1.8 keV at 1332 keV of  ${}^{60}\text{Co}$  and 50% relative efficiency) coupled to a 2048- and/or 4096-channel pulse-height analyzer. The excellent energy resolution of the HPGe detector resulted in a good signal-to-noise ratio. The background was reduced by a lead shield. Therefore, the background peaks do not impair the determination of the half-life of  ${}^7\text{Be}$  in the present experiment. The radioactivities associated with the decay of  ${}^7\text{Be}$  could be uniquely detected through the identification of its characteristic  $\gamma$ -rays, and all other sources could be ruled out.

We exactly set the measurement duration for one data point to 21600 s (6 hours), (exactly 21480 s for the live measurement time and 120 s for the dead time of the measurement system plus the sample exchange time and the waiting time to the next step). This procedure was repeated more than 300 times (over 150 days). Total measuring time was more than 150 days, which is almost three half-lives of  ${}^7\text{Be}$ . The internal clock time of a computer for data acquisition was always calibrated by a time-standard signal distributed via a long-wave radio center in Japan (i.e. the starting time for each run was correlated to a time distributed publicly). Therefore, the uncertainty in the time measurements is negligibly small. The system was completely controlled by a computer to obtain precise measurement positions.

The reproducibility of each position was determined to be within 0.05 mm. Systematic errors were reduced by using the Be metal( ${}^7\text{Be}$ ) as a reference. To keep the constancy of a geometrical factor between the sources and the  $\gamma$ -ray detector, the temperature was kept at 20 °C by air conditioner during the measurement.

### 3. Results and Discussion

A typical  $\gamma$ -ray spectrum obtained in a measurement of  ${}^7\text{Be}@C_{60}$  decay as a function in keV is shown in Figure 8. The expected  $\gamma$  line at  $E_\gamma=478$  keV and a natural background line at  $E_\gamma=1461$  keV can be seen as two giant peaks. No peak was seen at around  $E_\gamma=478$  keV when the  ${}^7\text{Be}$  sources were absent. A direct summation method, which is normally used for a neutron activation analysis etc, was applied to obtain the peak area ( $E_\gamma=478$  keV). The background was subtracted by a straight line between the average counting number/channel on both sides of the peak. In Figure 9, the two measured exponential decay curves for the  ${}^7\text{Be}@C_{60}$  and Be metal( ${}^7\text{Be}$ ) activities are plotted versus time. Closed circles and cross symbols, respectively, indicate the radioactivities (decay rate) of the  ${}^7\text{Be}@C_{60}$  and Be metal( ${}^7\text{Be}$ ) samples. The initial radioactivities of the  ${}^7\text{Be}$  in each sample were almost identical, i.e. at time zero we obtained around 2.7 counts per second (cps) for  ${}^7\text{Be}@C_{60}$  and 2.5 cps for Be metal( ${}^7\text{Be}$ ) in one run. Thus, the two decay curves can be compared under almost the equal degree in count rate (cps). The data for Be metal( ${}^7\text{Be}$ ) shown in Figure 9 was normalized to those for  ${}^7\text{Be}@C_{60}$  by use of an adjustment procedure on initial points of the two decay curves. The decay constant for the two samples were obtained by fitting straight lines in logarithm for the vertical line to the measured data points by use of the MINUIT program distributed from the CERN Program Library. This program takes into account the statistical errors associated with each data point in Figure 9. This statistical error is by far the dominating uncertainty. The uncertainty of our measurement is given by the uncertainty of the slope of the straight line fitted to the logarithm of the counts. We have measured the decay rates and deduced the corresponding half-lives of  ${}^7\text{Be}$  in the  ${}^7\text{Be}@C_{60}$  and in the Be metal( ${}^7\text{Be}$ ) samples in two separate measurements for each

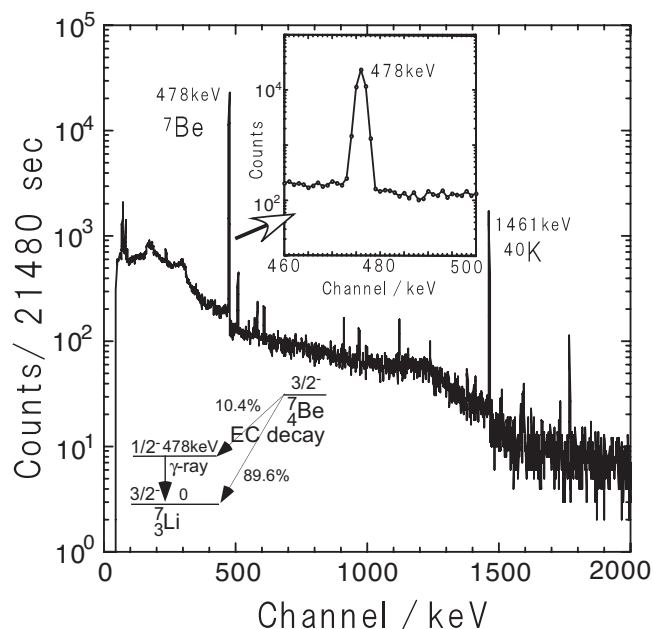


**Figure 8.** Typical  $\gamma$ -ray spectrum of  ${}^7\text{Be}$  in the  ${}^7\text{Be}@C_{60}$  fraction. Expanded scale around the  $E_\gamma=478$  keV is shown in the figure. Decay scheme of  ${}^7\text{Be}$  is inserted in the figure.

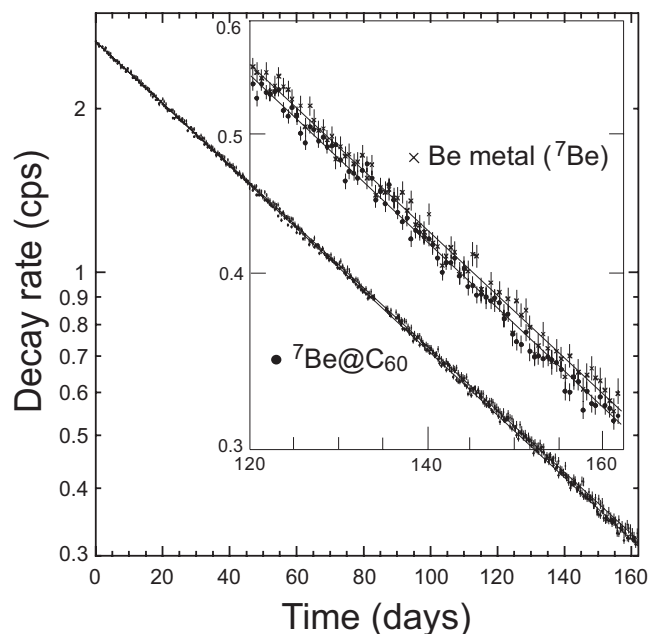


**Figure 9.** Exponential decay curves of  ${}^7\text{Be}$  in the samples of  ${}^7\text{Be}@C_{60}$  and Be metal( ${}^7\text{Be}$ ). Inset figure corresponding to the decay intervals of 120~162 days are displayed with an expanded scale.

sample in duration more than 150 days. The averaged results for the samples of the  ${}^7\text{Be}@C_{60}$  and Be metal( ${}^7\text{Be}$ ) are  $T_{1/2}=52.65\pm 0.04$ , and  $T_{1/2}=53.25\pm 0.04$  days, respectively. The reduced  $\chi$ -square values of the exponential fits are between 0.90 and 1.20. The dead time in the data acquisition system has been found to be about 8~15 s for each 21480 s run. Therefore, the uncertainty due to the dead time was estimated to be less than 0.04%, and the systematic error in the measurements was estimated to be less than half of the statistical error quoted above.<sup>43</sup> (In order to reduce the dead time of the measurement system, the amount of the activities and the distance between a  $\gamma$ -ray detector and the source were prepared suitably in the measurement.)

The counting rates of the natural background, which consist of the 1461 keV  $\gamma$ -rays emanating from  ${}^{40}\text{K}$ , were also analyzed. The data for  ${}^{40}\text{K}$  obtained were fitted by the same procedures

using the NIMUIT program. It was found that the fitted line closely corresponded to a horizontal line. Therefore, the present decay rates for the samples of the  $^7\text{Be}@C_{60}$  and Be metal( $^7\text{Be}$ ) seem to be fair.

In Figure 10, solid circles indicate the half-lives obtained for the  $^7\text{Be}@C_{60}$  sample compared with that for the Be metal( $^7\text{Be}$ ) given by cross symbols. It was surprising to observe that the half-life obtained for  $^7\text{Be}$  in the sample  $^7\text{Be}@C_{60}$ ,  $T_{1/2}=52.65\pm 0.04$  days, was as much as 1.13% shorter than that for the Be metal( $^7\text{Be}$ ) sample, where we define the percentage difference by  $[100(\lambda(C_{60})-\lambda(\text{Be metal}))/\lambda(\text{Be metal})]$ . This difference in half-lives is sufficiently large that it is clearly discernable when the data is displayed on the extended scale of the right inserted figure in Figure 9. The half-life of  $^7\text{Be}$  inside  $C_{60}$  is shorter than that in any previously reported in environments for any materials and/or pressure. This implies that the  $^7\text{Be}$  atoms are located in a unique environment inside the  $C_{60}$  cages.

On the other hand, the half-life of  $^7\text{Be}$  in the Be metal( $^7\text{Be}$ ) averaged over many measurements was  $53.25\pm 0.04$  days.<sup>47</sup> The half-lives obtained for  $^7\text{Be}$  in several other host materials and chemical forms such as graphite, gold, oxide, etc. have been presented by many researchers.<sup>10-18,20-26</sup> In Figure 10, the half-lives previously measured are also shown by the range of a thick bar as a comparison. Here, only the half-lives obtained using a standard time distributed publicly (stated in the text) are considered.<sup>10,13-15,17,18</sup> The half-lives inside the values are mostly between 53.10 and 53.40 days. For example, the half-life values obtained for  $^7\text{Be}$  in several other host materials such as graphite and boron nitride that have been presented by Jaeger et al<sup>10</sup> and Norman et al,<sup>14</sup> respectively, are also shown in Figure 11. The values are almost all in the range of 53.1 to 53.3 days.<sup>14</sup> Therefore, we found that our reference measurement of the half-life for  $^7\text{Be}$  in the Be metal( $^7\text{Be}$ ) was in satisfactory agreement with the other available data.

Several factors have contributed to creating this unique environment, for example, the many  $\pi$  electrons of  $C_{60}$  and the special dynamic conditions of the electrons inside the  $C_{60}$  cage, which include the ratchet and/or tumbling motion,<sup>41,42</sup> all of which may affect the contact electron density at the  $^7\text{Be}$  nucleus. Here, a magnitude of the average charge-transfer from 2s electrons of the  $^7\text{Be}$  atom, e.g. the K and L capture,<sup>12,48,49</sup> can play an important role for such a large variation in the EC decay rate of  $^7\text{Be}$  between the samples of the  $^7\text{Be}@C_{60}$  and Be metal( $^7\text{Be}$ ). The L/K capture ratio (i.e. the ratio of the electron density of L(2s) and K(1s) orbitals at the Be nucleus position) is estimated to be almost 10% on an isolated Be atom.<sup>49,50</sup> In theoretical calculations, we also found that the  $^7\text{Be}$  atom stays at the center (potential minimum) of the  $C_{60}$  cage and the 2s electrons can be fully restricted to the Be nucleus at  $T=0$  K as if they were an isolated Be atom ( $1s^2 2s^2$ ).<sup>48</sup> A schematic view of the closed electron shells ( $1s^2 2s^2$ ) when  $^7\text{Be}$  is inside  $C_{60}$  is shown in Figure 12. On the other hand, chemically and/or metallicly bonded Be atoms have always lost the 2s electrons to some degree due to the alkaline-earth metal nature (relatively smaller electronegativity). Therefore, the L/K capture ratio in the  $^7\text{Be}$  atom is reduced when the  $^7\text{Be}$  is chemically bonded and/or inside the host metal materials. Here, the magnitude of the average charge-transfer from the L(2s) electrons of the  $^7\text{Be}$  atom may play an important role in such variation in the decay constant in the environments, though the K(1s) electrons may also play a large influence on the factor of the environments around the  $^7\text{Be}$  nuclear position. It is our hope that our results will stimulate further experimental and theoretical studies leading to a more quantitative understanding of this large change in the decay constant.

Finally, a dynamic motion inside  $C_{60}$  at room temperature may contribute to the environment around the  $^7\text{Be}$  nucleus. Therefore, it is intriguing to study the temperature dependence

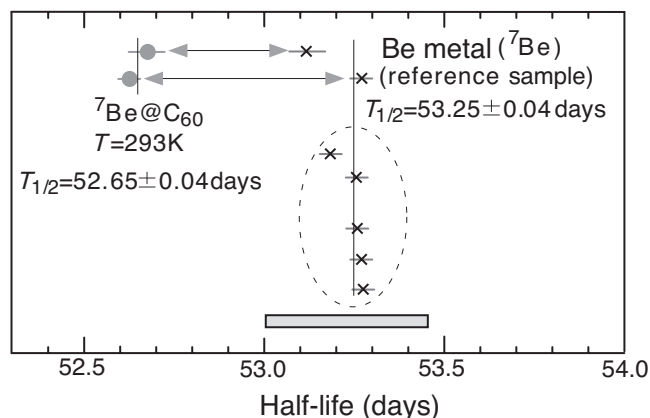


**Figure 10.** Half-lives ( $T_{1/2}$ ) measured in this time period are plotted as solid circles for the  $^7\text{Be}@C_{60}$ . The cross symbols represent the half-lives used as reference samples of Be metal( $^7\text{Be}$ ) (e.g. shown by arrows). The dashed area are the half-lives of the Be metal( $^7\text{Be}$ ) samples compared to other samples.<sup>47</sup> Half-lives previously presented mostly range inside the thick-bar.

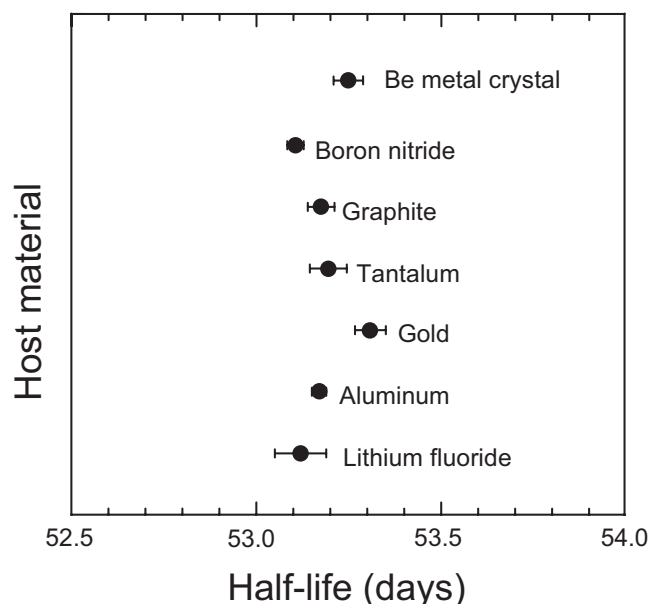


**Figure 11.** Half-life of  $^7\text{Be}$  in Be metal and half-lives previously measured in several host materials.<sup>10,14</sup>

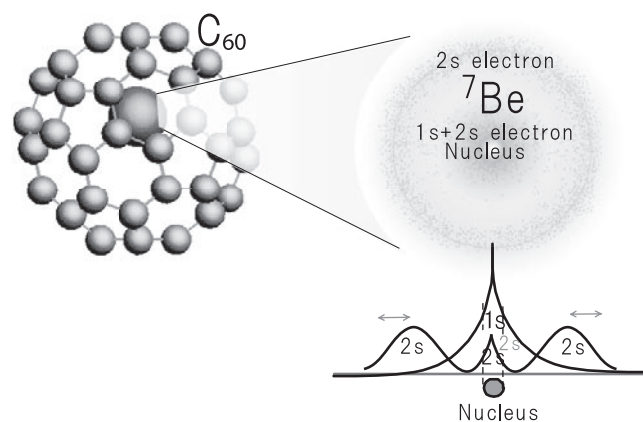


**Figure 12.** Schematic view of electron shell structure of  $^7\text{Be}$  inside  $C_{60}$ .

of the half-life of  $^7\text{Be}$  inside  $C_{60}$ . In our study, in order to suppress the dynamic motion of  $^7\text{Be}$  inside  $C_{60}$ , we are planning to measure the half-life of  $^7\text{Be}$  inside  $C_{60}$  that is cooled to a temperature close to liquid helium ( $T=5$  K). Now we are also carrying out calculations of the electron density at the  $^7\text{Be}$  nucleus

position at the site inside  $C_{60}$  by different temperatures (at  $T=0$  K and 293 K). The theoretical estimates will reveal the stable position of the  ${}^7\text{Be}$  nucleus inside  $C_{60}$  and the temperature dependence of the electron density at the  ${}^7\text{Be}$  nuclear position.

#### 4. Conclusion

In summary, we have measured the half-life of (1)  ${}^7\text{Be}$  encapsulated in  $C_{60}$  and (2)  ${}^7\text{Be}$  incorporated in Be metal using an HPGe detector with a time reference from a standard-time radio signal. We found that the half-life of  ${}^7\text{Be}$  inside  $C_{60}$  and in Be metal were  $T_{1/2}=52.65\pm 0.04$  and  $T_{1/2}=53.25\pm 0.04$  days, respectively. This 1.13% difference between the EC decay rate inside  $C_{60}$  and in Be metal represents a strong environmental effect on the  ${}^7\text{Be}$  EC decay rate, caused by the different electronic wave-functions near the  ${}^7\text{Be}$  nucleus inside a  $C_{60}$  cage and inside Be metal. These findings may give a fundamental understanding of the EC decay problem and/or hyperfine interactions. Extreme pressures and/or plasma states in stellar environments are supposed to change the EC decay rate by orders of magnitude. However, our more limited observed effects have still significantly raised the magnitude of what is achievable in laboratories on earth.

**Acknowledgement.** This research work was carried out by the collaborators, M. Muto, J. Kasagi, and H. Yuki in Laboratory of Nuclear Science of Tohoku University, T. Morisato in Accelrys K.K. Tokyo, Y. Kawazoe, T. Mitsugashira at the Institute of Materials Research of Tohoku University, The authors are grateful to the  ${}^{229m}\text{Th}$  collaboration for the continuous support (the list includes T. Nakanishi and T. Kikunaga of Kanazawa University, S. Shibata and K. Takamiya of Kyoto University, A. Shinohara and Y. Kasamatsu of Osaka University, H. Haba and T.T. Inamura of RIKEN, M. Hara of Tohoku University, and other all colleagues). The authors are also grateful to K. Endo for his kindness and K. Sakamoto and I. Fujiwara for the special attention to this work. We also acknowledge the valuable discussions and support by P. Möller (LANL), K. Masumoto (KEK), and K. Shikano (Hakodate). We convey our special thanks to the staff in the division of accelerators of the Laboratory of Nuclear Science and the Cyclotron and Radioisotope Center, Tohoku University. Finally, the authors appreciate the kindness of H. Nakahara of Tokyo Metropolitan University, who gave thoughtful and continuous advice on this work. This work was supported by Grant-in-Aids for Co-operative Research No.10640535, No.12640532, No.17350024 from the Ministry of Education of Japan, by the REIMEI Research Resources of Japan Atomic Energy Research Institute, and by MITSUBISHI Fund.

#### References

- (1) E. Segré, *Phys. Rev.* **71**, 274 (1947).
- (2) E. Segré and C.E. Wiegand, *Phys. Rev.* **75**, 39 (1949).
- (3) R.F. Leininger, E. Segré, and C. Wiegand, *Phys. Rev.* **76**, 897 (1949).
- (4) C. S. Cook, *Am. J. Phys.* **19**, 37 (1951).
- (5) R. Bouches, R. Daudel, P. Daudel, and R. Muxart, *J. Phys. Radium* **8**, 201 (1947).
- (6) R. Bouches, R. Daudel, P. Daudel, R. Muxart, and A. Rogozinski, *J. Phys. Radium* **10**, 201 (1949).
- (7) P. Benoist, R. Bouchez, P. Daudel, R. Daudel, and A. Rogozinski, *Phys. Rev.* **76**, 1000 (1949).
- (8) J.J. Kraushaar, E.D. Wilson, and K.T. Bainbridge, *Phys. Rev.* **90**, 610 (1953).
- (9) R. Bouches, J. Tobailem, J. Robert, R. Muxart, R. Mellet, P. Daudel, R. Daudel, R. Muxart, and A. Rogozinski, *J. Phys. Radium* **17**, 363 (1956).
- (10) M. Jaeger, S. Wilmes, V. Kollé, G. Staudt, and P. Mohr, *Phys. Rev. C* **54**, 423 (1996).
- (11) A. Ray, P. Das, S.K. Saha, S.K. Das, B. Sethi, A. Mookerjee, C.B. Chaudhuri, and G. Pari, *Phys. Lett.* **B 455**, 69 (1999).
- (12) A. Ray, P. Das, S.K. Saha, and S.K. Das, *Phys. Lett.* **B 531**, 187 (2002).
- (13) A. Ray, P. Das, S. K. Saha, S. K. Das, J. J. Das, N. Madhavan, S. Nath, P. Sugathan, P. V. M. Rao, and A. Jhingan, *Phys. Rev. C* **73**, 034323 (2006).
- (14) E.B. Norman, G.A. Rech, E. Browne, R.M. Larimer, M.R. Dragowsky, Y.D. Chan, M.C.P. Isaac, R.J. McDonald, and A.R. Smith, *Phys. Lett.* **B 519**, 15 (2001).
- (15) Z.Y. Liu, C.B. Li, S.G. Wang, J. Zhou, Q.Y. Meng, S.J. Lu, and S.H. Zhou, *Chinese Phys. Lett.* **20**, 829 (2003).
- (16) S.H. Zhou, Z.Y. Liu, J. Zhou, Q.Y. Meng, C.B. Li, G. Lian, B.X. Wang, and X.X. Bai, *Chinese Phys. Lett.* **20**, 829 (2003).
- (17) B. N. Limata, Zs. Fulop, D. Schurmann, N. De Cesare, A. D'Onofrio, A. Esposito, L. Gialanella, Gy. Gyurky, G. Imbriani, F. Raiola, V. Roca, D. Rogalla, C. Rolfs, M. Romano, E. Somorjai, F. Strieder, and F. Terrasi, *Eur. Phys. J. A* **27**, 193 (2006).
- (18) Y. Nir-El, G. Haquin, Z. Yungreiss, M. Hass, G. Goldring, S. K. Chamoli, B. S. Nara Singh, S. Lakshmi, U. Koster, N. Champault, A. Dorsival, G. Georgiev, V. N. Fedoseyev, B. A. Marsh, D. Schumann, G. Heidenreich, and S. Teichmann, *Phys. Rev. C* **75**, 012801(R) (2007).
- (19) V.N. Kondratyev and A. Bonasera, *Phys. Rev. Lett.* **74**, 2824 (1995).
- (20) C.A. Huh, *Earth Planet. Sci. Lett.* **171**, 325 (1999).
- (21) H.W. Johlige, D.C. Aumann, and H.J. Born, *Phys. Rev. C* **2**, 1616 (1970).
- (22) J.A. Tossell, *Earth Planet. Sci. Lett.* **195**, 131 (2002).
- (23) F. Lagoutine, J. Legrand, and C. Bac, *J. Appl. Radiat. Isot.* **26**, 131 (1975).
- (24) W.K. Hensley, W.A. Bassett, and J.R. Huizenga, *Science* **181**, 1164 (1973).
- (25) L. Liu and C.A. Huh, *Earth Planet. Sci. Lett.* **180**, 163 (2000).
- (26) W. B. Gogarty, *Naval Research Tec. Rep.* **7** (1963).
- (27) G.T. Emery, *Ann. Rev. Nucl. Sci.* **22**, 165 (1972).
- (28) H.W. Kroto, J.R. Heath, S.C. O'Brien, R.F. Curl, and R.E. Smalley, *Nature* **318**, 162 (1985).
- (29) W. Krätschmer, L.D. Lamb, K. Fostiropoulos, and D.R. Huffman, *Nature* **347**, 354 (1990).
- (30) Y. Chai, T. Guo, C. Jin, R.E. Haufler, L.P.F. Chibante, J. Fune, L. Wang, J.M. Alford, and R.E. Smalley, *J. Phys. Chem.* **95**, 7564 (1991).
- (31) M. Takata, B. Umeda, E. Nishibori, M. Sakata, Y. Saito, M. Ohno, and H. Shinohara, *Nature* **377**, 46 (1995).
- (32) M. Saunders, R.J. Cross, H.A. Jimenez-Vazquez, R. Shimshi, and A. Khong, *Science* **271**, 1693 (1996).
- (33) T. Braun and H. Rausch, *Chem. Phys. Lett.* **237**, 443 (1995).
- (34) G.E. Gadd, P. Schmidt, C. Bowles, G. McOrist, P.J. Evans, J. Wood, L. Smith, A. Dixon, and J. Easey, *J. Am. Chem. Soc.* **120**, 10322 (1998).
- (35) T. Ohtsuki, K. Masutomo, K. Sueki, K. Kobayashi, and K. Kikuchi, *J. Am. Chem. Soc.* **117**, 12869 (1995).
- (36) T. Ohtsuki, K. Masumoto, K. Ohno, Y. Maruyama, Y. Kawazoe, K. Sueki, and K. Kikuchi, *Phys. Rev. Lett.* **77**, 3522 (1996).
- (37) T. Ohtsuki, K. Ohno, K. Shiga, Y. Kawazoe, Y. Maruyama, and K. Masumoto, *Phys. Rev. Lett.* **81**, 967 (1998).
- (38) T. Ohtsuki, K. Ohno, K. Shiga, Y. Kawazoe, Y. Maruyama, and K. Masumoto, *J. Chem. Phys.* **112**, 2834 (2000).
- (39) T. Ohtsuki and K. Ohno, *Phys. Rev.* **72**, 153411 (2005).
- (40) K. Kobayashi, S. Nagase, and T. Akasaka, *Chem. Phys. Lett.* **261**, 502 (1996).

- (41) B.W. Smith, D.E. Luzzi, and Y. Achiba, *Chem. Phys. Lett.* **331**, 137 (2000).
- (42) W. Sato, K. Sueki, K. Kikuchi, K. Kobayashi, S. Suzuki, Y. Achiba, H. Nakahara, Y. Ohkubo, F. Ambe, and K. Asai, *Phys. Rev. Lett.* **80**, 133 (1998).
- (43) T. Ohtsuki, H. Yuki, M. Muto, J. Kasagi, and K. Ohno, *Phys. Rev. Lett.* **93**, 112501 (2004).
- (44) K. Ohno, Y. Maruyama, and Y. Kawazoe, *Phys. Rev.* **B 53**, 4078 (1996).
- (45) K. Ohno, Y. Maruyama, K. Esfarjani, Y. Kawazoe, N. Sato, R. Hatakeyama, T. Hirata, and M. Niwano, *Phys. Rev. Lett.* **76**, 3590 (1996).
- (46) C.M. Lederer and V.S. Shirley, eds, *Table of Isotopes*, 8th Ed. Vol. I, John Wiley & Sons, Inc. 1996.
- (47) T. Ohtsuki, K. Ohno, T. Morisato, and K. Hirose, *Materials Transactions* **48**, 646 (2007).
- (48) T. Morisato, K. Ohno, and T. Ohtsuki, to be published.
- (49) P. A. Voytas<sup>1</sup>, C. Ternovan<sup>1</sup>, M. Galeazzi, D. McCammon, J. J. Kolata, P. Santi, D. Peterson, V. Guimaraes, F. D. Becchetti, M. Y. Lee, T. W. O'Donnell, D. A. Roberts, and S. Shaheen, *Phys. Rev. Lett.* **88**, 012501 (2002).
- (50) A. Ray, P. Das, S.K. Saha, S.K. Das, and A. Mookerjee, *Phys. Rev.* **C 66**, 012501(R) (2002).

